Resistivity Anisotropy and Resistivity under Biaxial Strain in $CeRh_2As_2$

Robert Mehlig[1,3], Konstantin Semeniuk[2], Elena Hassinger[1,2]

[1]Dresden University of Technology, [2]Max Planck Institute of Chemical Physics of Solids, [3]Uppsala University

Resistivity Anisotropy — Motivation

$CeRh_2As_2$ is an actively studied unconventional superconductor. Despite a steady improvement in the quality of available crystals, the residual resistivity remains at a high value of *>30* μΩcm. Finding the dominant types of crystallographic defects may help with further improvements of crystal quality.

- **Key observation:** the residual resistivity ratio (*RRR*) is here defined as:

  $$RRR = \rho_{300\,K} / \rho_{0.5\,K}\,,$$

  and can be used as a measure of crystal quality. *RRR* correlates with the critical temperature of superconductivity (T_c) and a magnetic order (T_0).

  Crystallographic data indicates a larger uncertainty for the *c*-axis lattice constant [1].

- **Possible explanation:** stacking faults between closely related $CaBe_2Ge_2$- and $ThCr_2Si_2$-type structures could increase residual resistivity along the *c*-axis due to additional disorder.

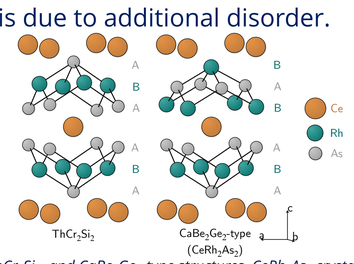

Fig. 1: *$ThCr_2Si_2$- and $CaBe_2Ge_2$-type structures. $CeRh_2As_2$ crystallizes in the $CaBe_2Ge_2$–type structure. After Fig. 1(a) in Ref. [2].*

- **Aim:** measure resistivity anisotropy to test this hypothesis (by comparing how RRR_{ab} and RRR_c change with crystal quality).

Method

Initial characterization: *RRR* values of pristine crystals from different batches were obtained.

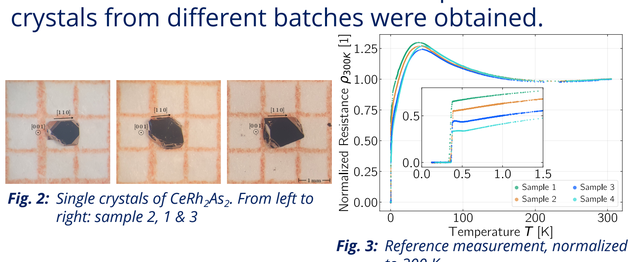

Fig. 2: *Single crystals of $CeRh_2As_2$. From left to right: sample 2, 1 & 3*

Fig. 3: *Reference measurement, normalized to 300 K.*

- **Microstructuring:** lamellae are made using Xe-plasma focused ion-beam (FIB) milling. They are then placed on sapphire substrates, anchored by Pt deposition and Au/Ti layers sputtered on top. The Au/Ti layers are used for defining electrodes.

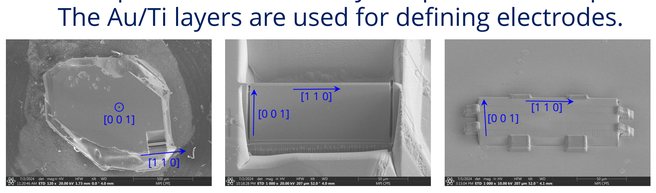

Fig. 4: *Stages of Xe-plasma FIB milling of Lamella.*

- **Device:** inside each lamella, a microstructure is milled to make a device for *c*- and *ab*-axis resistivity measurements. The design includes meandering paths for strain relief.

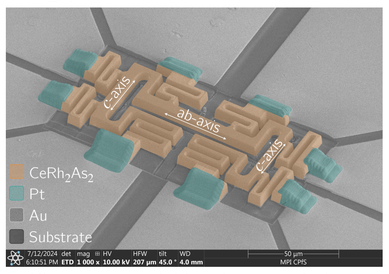

Fig. 5: *Microstructured resistivity-anisotropy device from sample 1.*

Key Results & Conclusions

- *ab*-plane resistivity is comparable to the reference measurement. *RRR* does not change after FIB exposure.

Batch ID.	RRR ($\rho_{300\,K}/\rho_{0.5\,K}$)			
	Bulk	*ab*-axis	*c*-axis (thin)	*c*-axis (wide)
Sample 1	1.504	1.441	1.176	1.189
Sample 2	1.793	1.832	1.493	1.507
Sample 3	2.242	2.475	1.856	1.898
Sample 4	2.990	–	–	–
	a-axis		*c*-axis	
Mishra, *et al.* [3]	2.351		1.543	

- Superconductivity and T_0 suppressed.

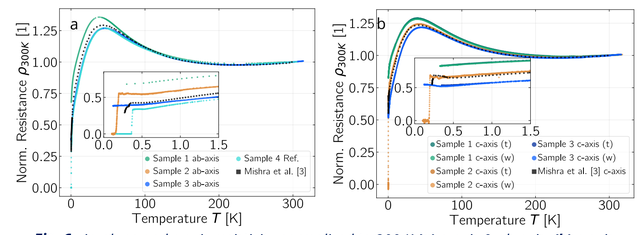

Fig. 6: *in-plane and c-axis resistivity normalized to 300 K **(a)** a-axis & ab-axis. **(b)** c-axis.*

- RRR_c and RRR_{ab} improve with crystal quality at a comparable rate. The suppression of T_c suggests that the effects of FIB irradiation or substrate-induced strain may be non-negligible.

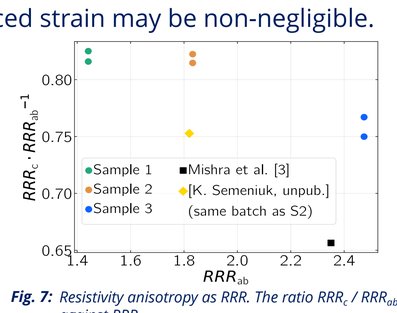

Fig. 7: *Resistivity anisotropy as RRR. The ratio RRR_c / RRR_{ab} against RRR_{ab}.*

Biaxial Strain — Motivation

Many strongly correlated electron systems can be effectively tuned via pressure or strain, but conventional strain cells are often impractical for sub-kelvin experiments due to size and thermalization issues. Substrate-induced strain offers a practical alternative.

- **Idea:** apply biaxial strain by gluing a polished crystal to a substrate, using differential thermal expansion during cooldown.
- **Substrate choice:** silicon for low thermal contraction and high stiffness ($E \approx 112$ GPa); estimated strain limit $\varepsilon_{max} \approx 0.28\%$.
- **COMSOL FEM:** simulated setup to estimate biaxial strain magnitude and distribution.
  - Predicted in-plane strain up to $\varepsilon_{max} \approx 0.29\%$, with a 15% variation near the probes and 3% through the crystal thickness at the center.

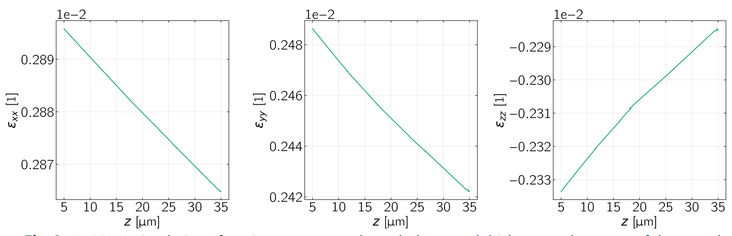

Fig. 8: *COMSOL simulation of strain components through the crystal thickness at the center of the crystal (z-direction). Geometry based on a crystal from batch 3.*

  - A high aspect ratio between the lateral size and thickness is required for homogeneous biaxial strain.

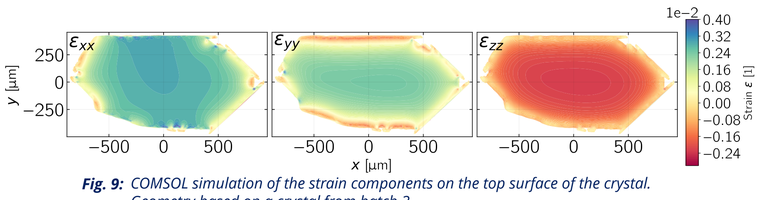

Fig. 9: *COMSOL simulation of the strain components on the top surface of the crystal. Geometry based on a crystal from batch 3*

Uncertainties & limitations: elastic constants of the crystal are placeholders ($E_{a,b} = 129$ GPa, $E_c = 109$ GPa) taken from [5], elastic constants of adhesive are taken from Stycast 2850FT ($E = 6.413$ GPa).

Method

- Crystals are polished using a hand-polishing jig.
- Optical profilometry is used to determine crystal height. Final thickness ≈*30* μm.

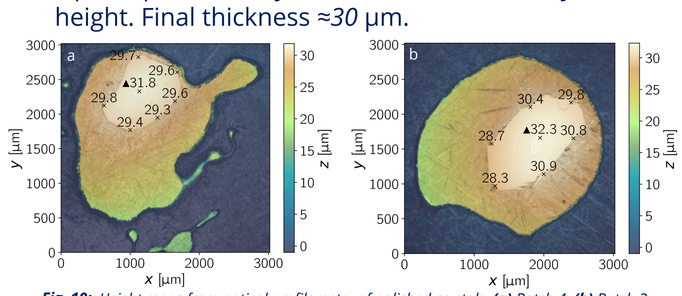

Fig. 10: *Height maps from optical profilometry of polished crystals. **(a)** Batch 4. **(b)** Batch 3.*

- The polished crystal is mounted to a substrate with Stycast 1266 epoxy.
- After curing, the crystal is cleaned and re-measured, giving an estimated adhesive thickness of *3–5* μm.

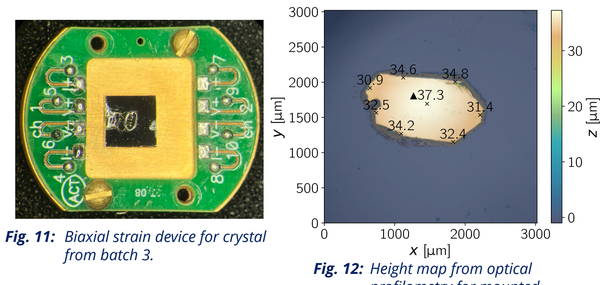

Fig. 11: *Biaxial strain device for crystal from batch 3.*

Fig. 12: *Height map from optical profilometry for mounted crystal from batch 3.*

Preliminary Results

- **Measurement:** superconductivity and T_0 suppressed; for $T > 0.75$ K there is no change in the temperature dependence of resistivity (compared to *ab*-axis).

Fig. 13: *Resistivity from biaxial strain measurement (batch 3) vs. reference and anisotropy data for same-batch crystals, normalized to 300 K.*

- **Conclusion:** established a feasible sample preparation protocol for applying substrate-induced biaxial strain. The observed effects were likely reduced due to poor strain transmission through the adhesive.

References:

[1] *P. Khanenko et al., "Phase diagram of $CeRh_2As_2$ for out-of-plane magnetic field", Phys. Rev. B, vol. 112, L060501 (2025).*

[2] *S. Khim et al., "Field-induced transition within the superconducting state of $CeRh_2As_2$". Science373, 1012-1016 (2021).*

[3] *S. Mishra et al., "Anisotropic magnetotransport properties of the heavy-fermion superconductor $CeRh_2As_2$". Phys. Rev. B 106, L140502 (2022).*

[4] *Maja D. Bachmann et al., "Spatial control of heavy-fermion superconductivity in $CeIrIn_5$". Science 366, 221-226 (2019).*

Funded by:

European Research Council
Established by the European Commission

MAX-PLANCK-INSTITUT FÜR CHEMISCHE PHYSIK FESTER STOFFE

TECHNISCHE UNIVERSITÄT DRESDEN

IFMP Institut für Festkörper- & Materialphysik